Vol 15 No 11, November 2006
1009-1963/2006/15(11)/2609-09

Chinese Physics

© 2006 Chin. Phys. Soc.
and IOP Publishing Ltd

Propagation properties of off-axis Hermite–cosh–Gaussian beam combinations through a first-order optical system

Tang Qian-Jin(唐前进)†, Chen Da-Ming(陈大明),
Yu Yong-Ai(于永爱), and Hu Qi-Quan(胡企铨)

Shanghai Institute of Optics and Fine Mechanics, Chinese Academy of Sciences, Shanghai 201800, *China*

(Received 10 November 2005; revised manuscript received 10 July 2006)

Based on the Collins integral formula, the analytic expressions of propagation of the coherent and the incoherent off-axis Hermite–cosh–Gaussian (HChG) beam combinations with rectangular symmetry passing through a paraxial first-order optical system are derived, and corresponding numerical examples are given and analysed. The resulting beam quality is discussed in terms of power in the bucket (PIB). The study suggests that the resulting beam cannot keep the initial intensity shape during the propagation and the beam quality for coherent mode is not always better than that for incoherent mode. Reviewing the numerical simulations of Gaussian, Hermite–Gaussian (HG) and cosh–Gaussian (ChG) beam combinations indicates that the Hermite polynomial exerts a chief influence on the irradiance profile of composite beam and far field power concentration.

Keywords: laser technology, beam propagation, beam combination, HChG
PACC: 4260, 6180D, 5240D, 9265R

1. Introduction

The beam combination is an available way to scale power and improve beam quality, so it has attracted much attention. Gas, solid state and fibre laser experiments have improved its feasibility in coherent and incoherent cases. Investigation of its propagation properties is also a significant research subject that can help to design and improve experiments.[1−3] Combining Gaussian, Hermite–Gaussian (HG) and cosh–Gaussian (ChG) beams with rectangular symmetry has been discussed already.[4−9] Recently, a new beam called Hermite–cosh–Gaussian (HChG) beam that is one of the solutions of the paraxial wave equation in a rectangular coordinate system was presented by Casperson and Tover.[10,11] It has been proved that the Gaussian and HG and ChG beams are the particular examples of HChG beam.[12] This new beam has been studied extensively, including parameters characterization and propagation properties.[13−16] Its combination characteristics, however, have not been investigated up to now. In the present paper, the propagation characteristics of HChG beams combination passing through a first-order optical system are studied in detail, which actually is a generalization of propagation properties of the beam combinations discussed previously.

†E-mail: tangqianjin@email.com

2. Physical model and derivation of closed-form expressions of propagation

Given that a rectangular laser array consists of $M \times N$ identical elements that are in HChG modes in the x-direction, and in Gaussian mode in the y-direction positioned at the plane $z = 0$, and the waist width of the TEM_{00} is ω_0. The separations between the elements are x_d and y_d, respectively, as shown in Fig.1.

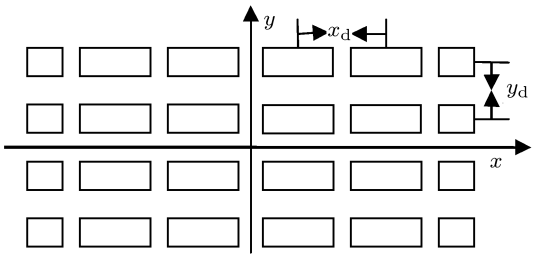


Fig.1. 2D mode of the $M \times N$ off-axis HChG beam array with rectangular symmetry.

Since the number of the array may be odd or even, M and N are set to be positive even in this paper. If we suppose that the initial phases of the beams are equal to zero, the field distributions of the beams at the input plane can be given by[10]

$$\begin{aligned} E_{mn}(x,y,0) =& H_p\left[\sqrt{2}\frac{(x-mx_{\rm d})}{\omega_0}\right] \\ & \times \exp\left[-\frac{(x-mx_{\rm d})^2+(y-ny_{\rm d})^2}{\omega_0^2}\right] \\ & \times \cosh\left[\Omega_0(x-mx_{\rm d})\right], \end{aligned} \tag{1}$$

$$m\in\left[-\frac{M-1}{2},\frac{M-1}{2}\right],\quad n\in\left[-\frac{N-1}{2},\frac{N-1}{2}\right],$$

where H_p denotes the Hermite polynomial of order p, and Ω_0 is the parameter associated with the cosh part, and the product $b=\Omega_0\omega_0$ is called the decentred parameter. When $b=0$, the pattern of HChG beam reduces to the familiar HG form, and for larger values of the coefficient, the cosh function plays a part in concentrating the energy into the outer lobes of the beam as illustrated by Fig.1 in Ref.[10].

The corresponding irradiance can be written as

$$\begin{aligned} I_{mn}(x,y,0) =& E_{mn}(x,y,0)E^*_{mn}(x,y,0) \\ =& H_p^2\left(\sqrt{2}\frac{(x-mx_{\rm d})}{\omega_0}\right) \\ & \times \exp\left[-\frac{2(x-mx_{\rm d})^2+2(y-ny_{\rm d})^2}{\omega_0^2}\right] \\ & \times \cosh^2\left[\Omega_0(x-mx_{\rm d})\right], \end{aligned} \tag{2}$$

where the symbol '*' denotes the complex conjugate.

The propagation of the beam described by Eq.(1) passing through a first-order optical system obeys the well-known Collins integral formula[17]

$$E_{mn}(x_1,y_1,z)=\frac{\mathrm{i}}{\lambda B}\iint E_{mn}(x,y,0)\exp\left\{-\frac{\mathrm{i}\kappa}{2B}\left[A(x^2+y^2)-2(xx_1+yy_1)+D(x_1^2+y_1^2)\right]\right\}\mathrm{d}x\mathrm{d}y, \tag{3}$$

where κ is the wave number related to the wavelength λ by

$$\kappa=2\pi/\lambda. \tag{4}$$

In fact, for convenience and simplicity a constant phase factor is omitted in Eq.(3) since it does not affect the relative intensity distribution of the beam. A, B, C and D are the elements of a transfer matrix on condition that $AD-BC=1$ for the complete optical system between the input and output planes.

Substituting Eq.(1) into Eq.(3), expressing the cosh function in the exponent form and recalling the integral formula[18]

$$\int_{-\infty}^{+\infty}\exp\left[-(x-y)^2\right]H_m(\alpha x)\mathrm{d}x=\sqrt{\pi}(1-\alpha^2)H_m\left(\frac{\alpha y}{\sqrt{(1-\alpha^2)}}\right), \tag{5}$$

one obtains

$$\begin{aligned} E_{mn}(x_1,y_1,z) =& \frac{1}{A+B/q_0}\left[\frac{Aq_0/B-1}{Aq_0/B+1}\right]^{p/2}H_p\left[\frac{\sqrt{2}(x_1-x_1d)}{\omega_x(z)}\right] \\ & \times \exp\left\{-\frac{\mathrm{i}\kappa}{2q_1}\left[(x_1-x_{1\rm d})^2+(y_1-y_{1\rm d})^2\right]-\mathrm{i}\kappa(\varepsilon_{1x}x_1+\varepsilon_{1y}y_1)+\mathrm{i}(\phi_x+\phi_y)\right\} \\ & \times \exp\left[\frac{b^2}{4(1+Aq_0/B)}\right]\cosh\left[\frac{b(x_1-x_{1d})}{A+B/q_0}\right], \end{aligned} \tag{6}$$

where $q_1(z)$ and q_0 are q complex parameters, which satisfy $ABCD$ law, i.e.

$$\frac{1}{q_1(z)}=\frac{C+D/q_0}{A+B/q_0},\quad q_0=\frac{\mathrm{i}\pi\omega_0^2}{\lambda}; \tag{7}$$

$$x_{1\rm d}=Amx_{\rm d},\quad \varepsilon_{1x}=Cmx_{1\rm d},\quad \phi_x=\frac{\kappa AC}{2}m^2x_{\rm d}^2; \tag{8}$$

$$y_{1\rm d}=Any_{\rm d},\quad \varepsilon_{1y}=Cny_{\rm d},\quad \phi_y=\frac{\kappa AC}{2}n^2y_{\rm d}^2; \tag{9}$$

$$\omega_1(z) = \omega_0 \left[A^2 - \left(B^2/q_0^2\right)\right]^{1/2}. \quad (10)$$

Equation (6) represents the propagation formula of off-axis HChG beams with rectangular symmetry in general. The formula can reduce to some particular cases, for example, when $b = 0$, it reduces to the expression of off-axis HG beam propagation;[5] when $p = 1$, one can obtain the ChG beam propagation;[6] if $b = 0$ and $p = 1$ are satisfied at the same time, the familiar off-axis Gaussian beam propagation can be obtained.[4]

As a particular case, the beams propagate through a thin lens with focal length f followed by a free space. The corresponding $ABCD$ matrix can be expressed as

$$\begin{pmatrix} A & B \\ C & D \end{pmatrix} = \begin{pmatrix} 1 & z \\ 0 & 1 \end{pmatrix} \begin{pmatrix} 1 & 0 \\ -1/f & 1 \end{pmatrix} = \begin{pmatrix} -\Delta z & f(1+\Delta z) \\ -1/f & 1 \end{pmatrix}, \quad (11)$$

where z is the propagation distance after the lens and Δz is determined by

$$\Delta z = \frac{(z-f)}{f}. \quad (12)$$

Substituting Eq.(11) into Eq.(6) yields

$$\begin{aligned} E_{mn}(x', y', \Delta z) =& \frac{\mathrm{i}\pi N_f}{1+\Delta z(1-\mathrm{i}\pi N_f)} \left[-\frac{1+\Delta z(1+\mathrm{i}\pi N_f)}{1+\Delta z(1-\mathrm{i}\pi N_f)}\right]^{p/2} H_p \left\{ \frac{\sqrt{2}\pi N_f \left(x' + \Delta z m x'_{\mathrm{d}}\right)}{\left[(1+\Delta z)^2 + (\pi N_f \Delta z)^2\right]^{1/2}} \right\} \\ & \times \exp\left\{ -\frac{\mathrm{i}\pi N_f(1-\mathrm{i}\pi N_f)}{1+\Delta z(1-\mathrm{i}\pi N_f)} \left[\left(x' + \Delta z m x'_{\mathrm{d}}\right)^2 + \left(y' + \Delta z n y'_{\mathrm{d}}\right)^2\right] + \mathrm{i}2\pi N_f \left(m x'_{\mathrm{d}} x' + n y'_{\mathrm{d}} y'\right) \right\} \\ & \times \exp\left\{ \left[\mathrm{i}\pi N_f \Delta z \left(m x'_{\mathrm{d}}\right)^2 + \left(n y'_{\mathrm{d}}\right)^2\right] + \frac{b^2(1+\Delta z)}{4\left[1+\Delta z(1-\mathrm{i}\pi N_f)\right]} \right\} \\ & \times \cosh\left[\frac{\mathrm{i}\pi N_f b \left(x' + \Delta z m x'_{\mathrm{d}}\right)}{1+\Delta z\left(1-\mathrm{i}\pi N_f\right)} \right], \end{aligned} \quad (13)$$

where the normalized parameters are determined as follows:

$$x' = \frac{x_1}{\omega_0}, \quad y' = \frac{y_1}{\omega_0}; \quad x'_{\mathrm{d}} = \frac{x_{\mathrm{d}}}{\omega_0}, \quad y'_{\mathrm{d}} = \frac{y_{\mathrm{d}}}{\omega_0}, \quad (14)$$

and the $N_f = \omega_0^2/\lambda f$ is the Fresnel number associated with the beam.

Now, the field profile of input beam at any propagation plane can be obtained from Eq.(13) with the normalized parameters. From the analytical expression one can find that, generally speaking, except at $\Delta z = 0$ plane the resulting beam profile is dependent on number of beams, the decentred parameter, the order of Hermite polynomial, the propagation distance and the separation between the beams.

3. Numerical examples and comparison analysis

Usually, there are two ways to combine beams, which are coherent and incoherent modes. For the incoherent case, the irradiance of the composite beam is described by

$$I(x, y, z) = \sum_m \sum_n E_{mn}(x, y, z) E^*_{mn}(x, y, z). \quad (15)$$

The calculation parameters are $M = 8$, $N = 4$, $N_f = 5$, $p = 4$, $x'_{\mathrm{d}} = y'_{\mathrm{d}} = 1.5$ and $b = 1.5$ unless otherwise stated. Figures 2 and 3 show the irradiances of the resulting beam at $\Delta z = -0.5$ and $\Delta z = -0.05$ for the incoherent case, respectively.

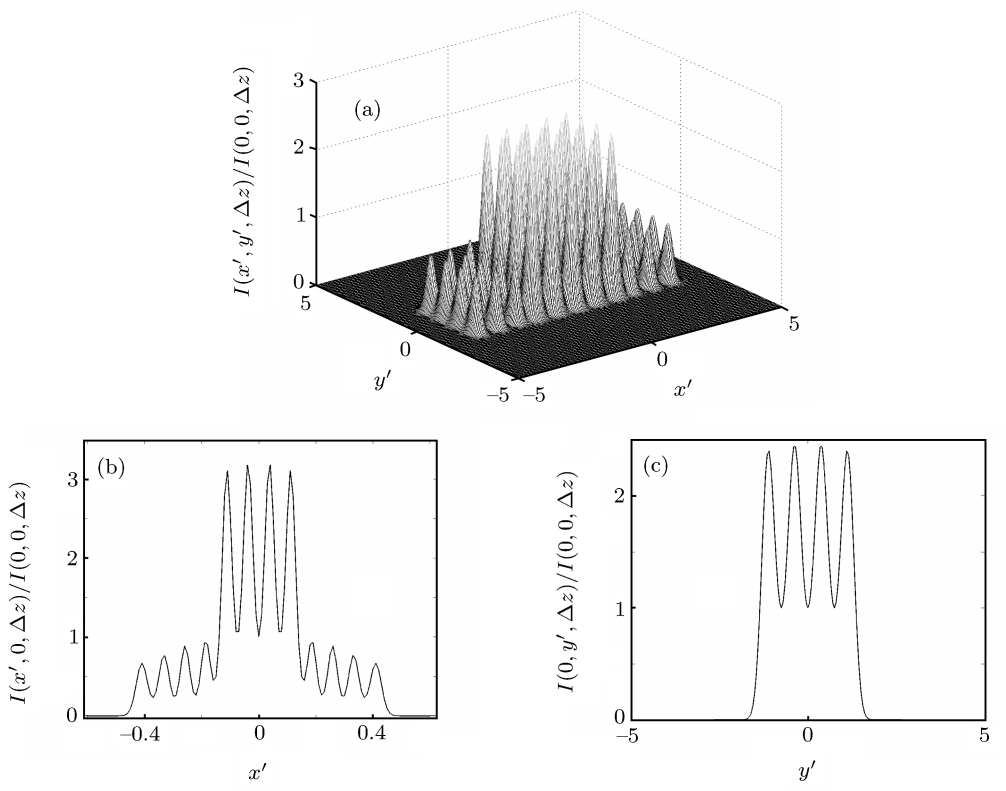


Fig.2. Relative irradiance profiles of resulting beam focused by a lens for the incoherent combination at $\Delta z = -0.5$. (a) $I(x', y', \Delta z)/I(0, 0, \Delta z)$ versus x' and y', (b) $I(x', y', \Delta z)/I(0, 0, \Delta z)$ versus x', (c) $I(x', y', \Delta z)/I(0, 0, \Delta z)$ versus y'.

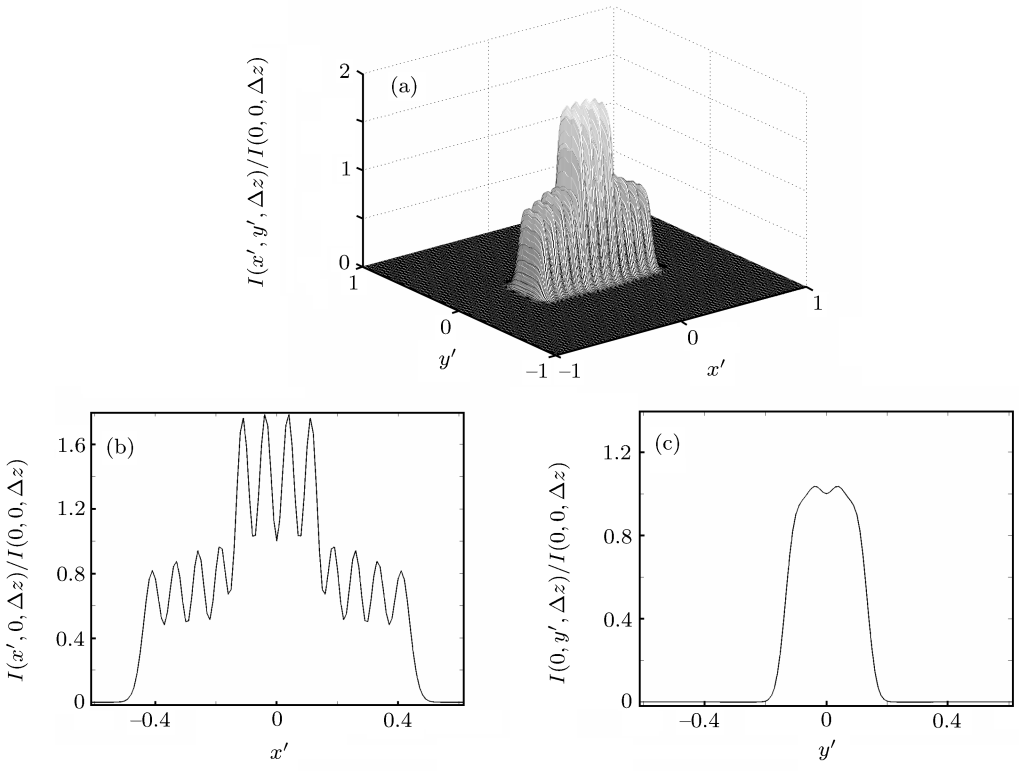


Fig.3. Relative irradiance profiles of resulting beam focused by a lens for the incoherent combination at $\Delta z = -0.05$. (a) $I(x', y', \Delta z)/I(0, 0, \Delta z)$ versus x' and y', (b) $I(x', y', \Delta z)/I(0, 0, \Delta z)$ versus x', (c) $I(x', y', \Delta z)/I(0, 0, \Delta z)$ versus y'.

In particular, the irradiance profile of the composite beam at the focal plane is simplified into

$$I(x', y', \Delta z = 0) = MN\pi^2 N_f^2 H_p^2 \left(\sqrt{2}\pi N_f x'\right) \exp\left[2\pi^2 N_f^2 \left(x'^2 + y'^2\right)\right] \cosh^2\left(\mathrm{i}\pi N_f b x'\right) \tag{16}$$

and the corresponding distributions are plotted against normalized coordinates in Fig.4.

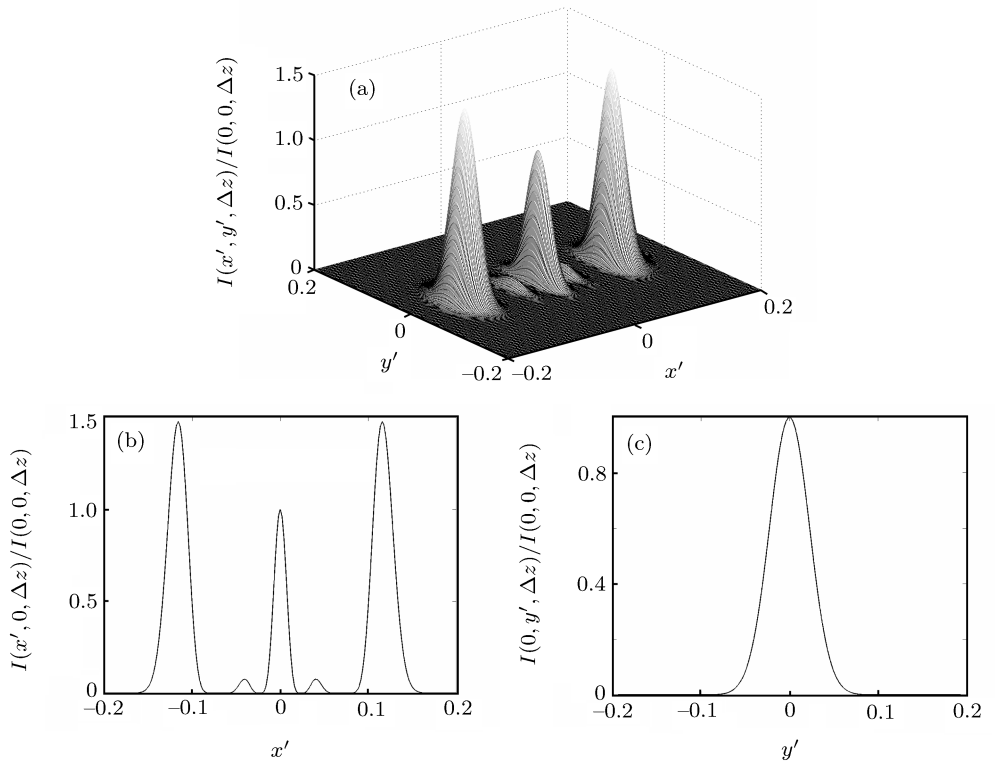


Fig.4. Relative irradiance profiles of resulting beam focused by a lens for the incoherent combination at $\Delta z = 0$. (a) $I(x', y', \Delta z)/I(0, 0, \Delta z)$ versus x' and y', (b) $I(x', y', \Delta z)/I(0, 0, \Delta z)$ versus x', (c) $I(x', y', \Delta z)/I(0, 0, \Delta z)$ versus y'.

For the coherent case, the irradiance of the composite beam is given by

$$I(x, y, z) = E(x, y, z)E^*(x, y, z), \tag{17}$$

where

$$E(x, y, z) = \sum_m \sum_n E(x, y, z). \tag{18}$$

When the parameters are the same as those of incoherent combination, and irradiance distributions of the resulting beam are shown in Figs.5 and 6.

In the far field, the expression of the irradiance of coherent combination can reduce to

$$\begin{aligned} I(x', y', \Delta z = 0) =& \pi^2 N_f^2 H_p^2 (\sqrt{2}\pi N_f x') \exp\left(-2\pi N_f x'\right) \cosh^2\left(\mathrm{i}\pi N_f b x'_{\mathrm{d}}\right) \\ & \times \frac{\left[1 - \cos(2\pi N_f m x'_{\mathrm{d}} x')\right]\left[1 - \cos(2\pi N_f n y'_{\mathrm{d}} y')\right]}{\left[1 - \cos(2\pi N_f x'_{\mathrm{d}} x')\right]\left[1 - \cos(2\pi N_f y'_{\mathrm{d}} y')\right]}. \end{aligned} \tag{19}$$

The corresponding intensity distributions are depicted in Fig.7.

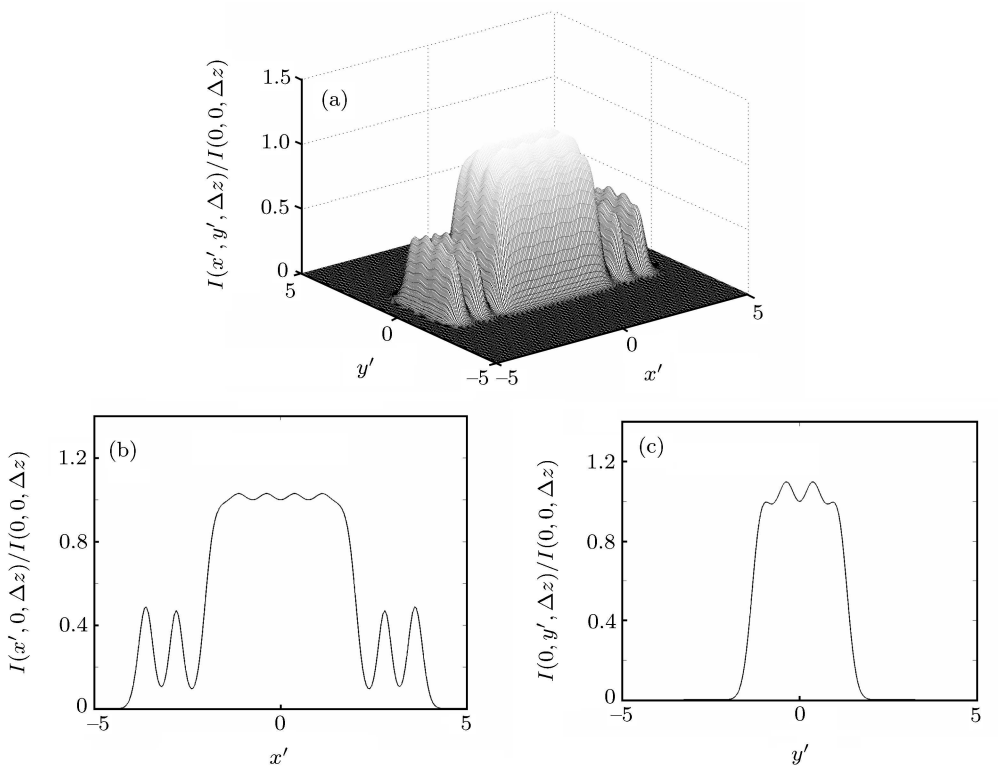


Fig.5. Relative irradiance profiles of resulting beam focused by a lens for the coherent combination at $\Delta z = -0.5$. (a) $I(x', y', \Delta z)/I(0, 0, \Delta z)$ versus x' and y', (b) $I(x', y', \Delta z)/I(0, 0, \Delta z)$ versus x', (c) $I(x', y', \Delta z)/I(0, 0, \Delta z)$ versus y'.

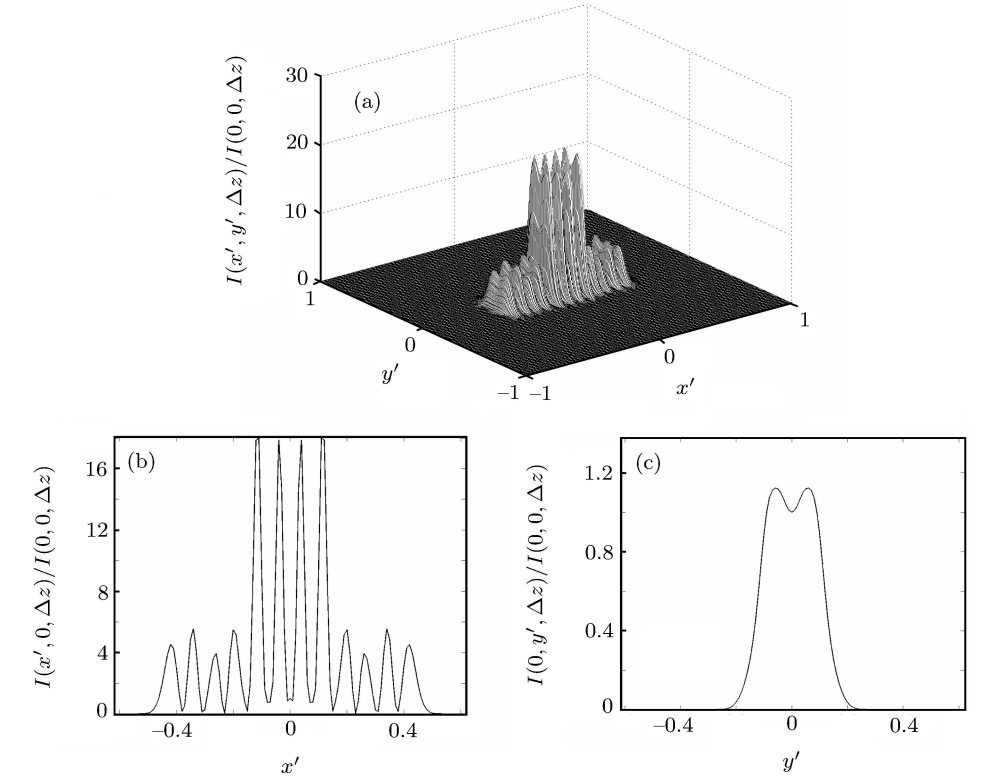


Fig.6. Relative irradiance profiles of resulting beam focused by a lens for the coherent combination at $\Delta z = -0.05$. (a) $I(x', y', \Delta z)/I(0, 0, \Delta z)$ versus x' and y', (b) $I(x', y', \Delta z)/I(0, 0, \Delta z)$ versus x', (c) $I(x', y', \Delta z)/I(0, 0, \Delta z)$ versus y'.

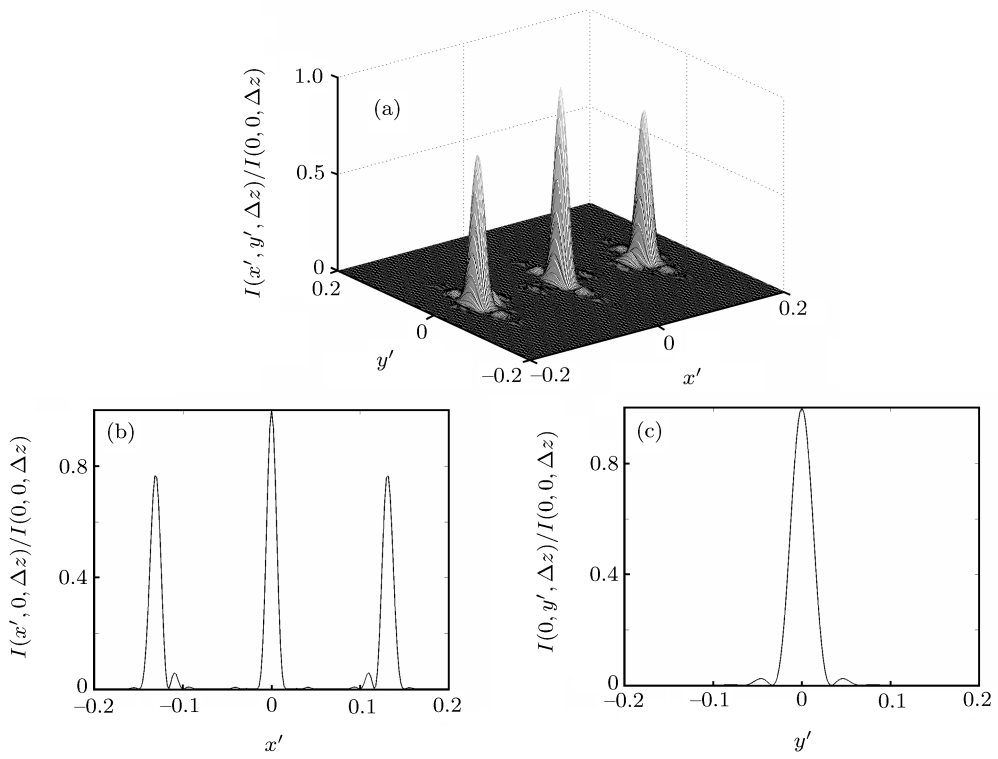


Fig.7. Relative irradiance profiles of resulting beam focused by a lens for the coherent combination at $\Delta z = 0$. (a) $I(x', y', \Delta z)/I(0, 0, \Delta z)$ versus x' and y', (b) $I(x', y', \Delta z)/I(0, 0, \Delta z)$ versus x', (c) $I(x', y', \Delta z)/I(0, 0, \Delta z)$ versus y'.

From Figs.2–3 and 5–7 it can be seen that the irradiance profiles of the resulting beams are changing during propagation and cannot preserve the HChG shape in the x'-direction and the Gaussian pattern in the y'-direction for both the coherent and incoherent cases at the planes $\Delta z = -0.5$ and –0.05, and for coherent combination mode at the focal plane. These propagation properties are similar to those of HG and ChG beam combinations.[4,6] For the incoherent composite beam at the focal plane as shown in Fig.4, the composite beam resembles a single HChG beam in the far field in shape as shown by Fig.1 in Ref.[10], three main lobes exist in the x'-direction and Gaussian-like in the y'-direction. Further, the irradiance profile is independent of separations x'_{d} and y'_{d} from Eq.(16), which can be explained by imaging principle of geometry optics. For the coherent composite beam, the irradiance profiles, for the most part, can keep a flat-top-like shape in the two directions from the input plane to $\Delta z = -0.35$; for the incoherent composite beam, the irradiance distribution, however, keeps HG shape only in the x'-direction. A comparison between the far field distributions illustrated in Figs.4(b) and 7(b) shows that there exist three main peaks in the x'-direction and the distance between the first and third peaks is almost equal but the intensity of the central peak is much larger than the intensities of the peaks on both sides for the coherent case, but the situation is inverse for the incoherent case. Figures 4(c) and 7(c) illustrate that though there exist two side lobes in the y'-direction for the coherent combination, the spot size is much small compared with that for the incoherent combination, so more energy concentrates into the central lobe as discussed in the next section. By reviewing the resulting profiles of HChG, ChG, HG and Gaussian beam combinations one can find that only if there exists the Hermite polynomial in the initial optical field, multiple lobes will occur during propagation. In other words, the Hermite polynomial term in the optical field is a chief factor leading to the occurrence of multiple peaks of composite beams and the deterioration of the beam quality, so preventing the Hermite term from occurring is necessary in order to obtain a high peak power and strong energy concentration.

4. Quality of the resulting beam

Usually, the M^2 factor and power in the bucket are used to characterize the beam quality, but it en-

counters some difficulty in measuring M^2 in a practical and readily way for the array beams.[19] Sometimes, it seems unreasonable to evaluate the resulting beam quality in terms of M-squared factor as indicated by the example given by Siegman.[20] The M^2 values of coherent and incoherent combinations of six Gaussian TEM_{00} beams arranged annularly are about 4.38 and 4.55, respectively, however, the six beams added together coherently can create a central lobe that is substantially narrower than that for the incoherent Gaussian case, with a central intensity being 6 times larger than that for the incoherent case on condition that total power is the same, so nothing can been gained by calculating M^2 of array additions. In fact, characterizing the beam quality of array with composite non-Gaussian beam profile in terms of M-squared factor is not practical nor the best way due to the fact that it is difficult to determine the beam width of beam profile.[21] In application, the engineers are interested in the power concentration on the target and how to measure the beam quality in a simple but accurate way, so the power in the bucket (PIB) curve is recommended to be used for characterizing the beam quality of non-Gaussian profile.[22] The PIB curve reveals the information about the transverse energy distribution and it is an easy method of practical measurement, for example, rectangularly scanning in the x- and y-directions using a knife edge.[20]

PIB is defined as the fraction of power within a given bucket's size in the far field and the corresponding expression reads

$$\mathrm{PIB} = \frac{\int_{-a}^{a}\int_{-b}^{b} I(x',y',0)\mathrm{d}x'\mathrm{d}y'}{\int_{-\infty}^{+\infty}\int_{-\infty}^{+\infty} I(x',y',0)\mathrm{d}x'\mathrm{d}y'}, \qquad (20)$$

with a and b being the normalized bucket's dimensions in the x'- and y'-directions, and $I(x',y',0)$ is given by Eq.(19) for coherent case and by Eq.(16) for incoherent case. Figure 8 indicates the PIB curves of beams after coherent and incoherent combinations in the x'- and y'- directions, the corresponding calculation parameters are the same as those of Figs.4 and 7. One can see from Fig.8(a) that the PIB for coherent case in the x'-direction is not always larger than that for incoherent case, which is similar to the case for HG beam combinations as shown by Fig.10 in Ref.[5]. The curve builds up much faster within 0.01 times the waist width for the coherent case because of the strong central lobe as plotted in Fig.7(c). It is also apparent, however, that the PIB of coherent combination is smaller than that of incoherent combination within the range of $0.11 < x' < 0.14$. In this direction, there exist three crossing points in the PIB curve, and the central lobe contains 42% of the total energy for the coherent combination while only 20% for the incoherent combination. Figure 8(b) shows that in the y'-direction the PIB of coherent combination is always larger than that of incoherent combination because there exists only Gaussian field in this direction. By reviewing the PIB curves of different mode structures,[4−6] one can conclude that the initial field distribution with Hermite polynomial leads the quality of resulting beam for coherent case not to be always larger than that for incoherent case, which is in agreement with the case for irradiance profile as discussed in Section 3.

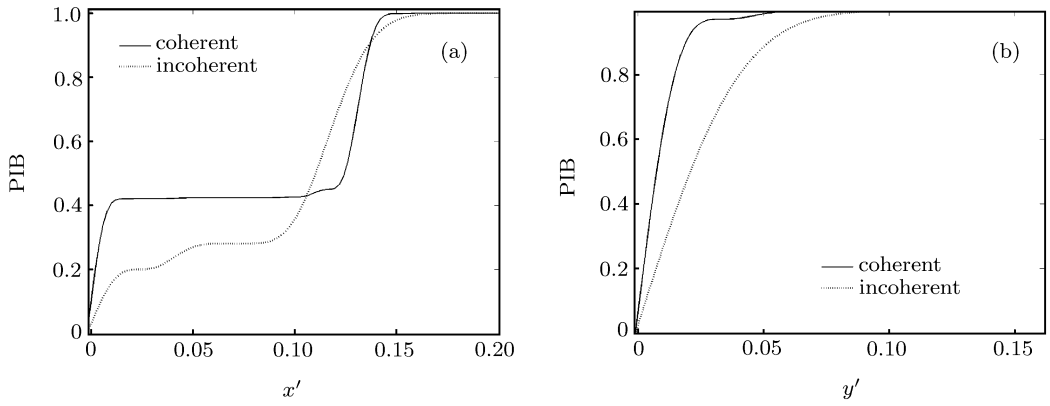


Fig.8. The PIB curves of resulting beam focused by a lens for the coherent combination and incoherent . (a) in the x'-direction and (b) in the y'-direction.

5. Conclusion

The coherent and the incoherent beam combinations of off-axis HChG beam with rectangular symmetry through a first-order optical system have been studied in detail. The analytical expression of composite beam propagation has been derived based on the generalized diffraction integral formula in the form of ABCD matrix, and corresponding numerical examples are demonstrated. The PIB curve is chosen to characterize the resulting beam quality. Reviewing the four mode structures, one concludes that beam quality of coherent combination is not always better than that of incoherent combination due to the existence of Hermite term in the initial optical field, that is to say, Hermite term of the initial field leads the beam quality to worsen for the coherent combination, so it is necessary to prevent the Hermite term from occurring by designing the resonator and pumped configuration. It should be noted that in this study the beams combining either coherently or incoherently is under the ideal condition, so partial coherent case is likely to occur in practice, which is deserving of further study.

Acknowledgments

The authors wish to express their heartfelt thanks to Dr Deng D M and Xiong H for helpful discussions.

References

[1] Ge D, Cai Y J and Lin Q 2005 *Chin. Phys.* **14** 128
[2] Wu P, Lü B D and Chen T L 2005 *Chin. Phys.* **14** 1130
[3] Peng Q J, Sun Z P, Chen Y H, Guo L, Bo Y, Yang X D and Xu Z Y 2005 *Opt. Lett.* **30** 1485
[4] Lü B D and Ma H 1999 *Opt. Commun.* **171** 185
[5] Lü B D and Ma H 2000 *Appl. Opt.* **39** 1279
[6] Deng D M 2004 *Phys. Lett.* A **333** 485
[7] Lü B and Ma H 2000 *Opt. Commun.* **178** 395
[8] Lü B and Ma H 2001 *J. Mod. Opt.* **48** 415
[9] Lü B D and Ma H 2000 *Opt. Commun.* **174** 99
[10] Casperson L W and Tover A A 1998 *J. Opt. Soc. Am.* A **15** 954
[11] Tover A A and Casperson L W 1998 *J. Opt. Soc. Am.* A **15** 2425
[12] Wang X Q and Lü B D 2002 *Acta Phys. Sin.* **51** 247 (in Chinese)
[13] Mei Z R, Zhao D M, Sun D and Gu J G 2004 *Optik* **115** 89
[14] Belafhal A and Ibnchaikh M 2000 *Opt. Commun.* **186** 269
[15] Yu S, Guo H, Fu X and Hu W 2002 *Opt. Commun.* **204** 59
[16] Zhou N R and Zeng G H 2004 *Opt. Commun.* **232** 49
[17] Collins S A 1970 *J. Opt. Soc. Am.* A **60** 1168
[18] Gradshteyn I S and Ryzhik I M 1980 *Table of Integrals, Series, and Products* (New York: Academic Press)
[19] Lü B D, Ji X L, Luo S R and Tao X Y 2004 *Infrared and Laser Eng.* **33** 14 (in Chinese)
[20] Siegman A E 1998 *OSA TOPS* **17** 184
[21] Yang C L 1996 *Laser J.* **17** 1 (in Chinese)
[22] Palma G E, Benda S S and Cunningham P R 1990 *Proc. SPIE* **1224** 202